Properties of Unidirectional Kenaf Fiber–Polyolefin Laminates

Sangyeob Lee,[1] Sheldon Q. Shi,[1] Leslie H. Groom,[2] Yibin Xue[3]
[1]*Department of Forest Products, Mississippi State University, Starkville, Mississippi 39762*

[2]*USDA Forest Service, Southern Research Station, Pineville, Louisiana 71360*

[3]*Department of Mechanical and Aerospace Engineering, Utah State University, Logan, Utah 84322*

The objective of this research was to evaluate the effect of kenaf fiber orientation and furnish formulation on the properties of laminated natural fiber–polymer composites (LNPC). The uniaxial fiber orientation provided property enhancement of the LNPC. The randomly oriented kenaf fibers, regardless of fiber contents in the laminates, provided an equal performance compared to the composites made of 25% fiber glass reinforced polyvinyl ester resin in the same laboratory processing conditions. Thermal properties of the laminates obtained from thermal gravimetry with differential scanning calorimetry (TG-DSC) showed that the melting point (T_m) of the polypropylene (PP) film laminates decreased, and the crystallization peak increased as the kenaf fiber content in the laminates increased. The surface morphology results of the kenaf fiber and fractures of the laminates showed that some fibers pulled out from the matrix. The mechanical properties increased as the kenaf fiber content increased. The tensile stress of the laminated composites fabricated with unidirectional fiber orientation was about 2–4 times higher than those with the randomly oriented samples. POLYM. COMPOS., 00:000–000, 2009. © 2009 Society of Plastics Engineers

INTRODUCTION

Polymeric materials have been successfully used in different industries including semiconductor, biomedical, automotive, and aerospace, because of their unique properties, such as resistant to abrasion, low heat conduction, low moisture absorption, and sufficient hardness and strength [1–3]. However, even though the polymer materials have excellent bulk physical, chemical, and weather resistance properties, their applications are limited because of the low surface energy and wettability. It is difficult to obtain a permanent bonding between the natural fibers and polymer matrices. Surface modifications such as chemical treatments, flame treatments, corona, plasma, UV light, ozone, and fluorination on the natural fibers or polyolefins are necessary [4–6] to obtain a satisfied interfacial adhesion. With these modification techniques, the surface characteristics of polymers and reinforced material are altered without affecting the polymer properties. However, these techniques may not be cost effective for mass production.

Natural fiber-reinforced polymer composites (NPC) have many advantages, including low cost, abundant resources, and high specific strength. These advantages are of interest to the industries that require materials of light weight, high performance to weight ratio, renewability, and minimum environmental impact [7–9]. The applications of NPC can be both non-structural and structural, such as decking, doors, window frames, flooring, fencing, walls, furniture, automobiles and electronic products [10, 11]. Natural fibers contain cellulose incorporated with hemicellulose and lignin, which contributes to the composite properties. In addition, the properties of natural fiber reinforced composites can be affected by the fiber geometry, content, distribution, orientation, and the fiber to matrix interface [2, 12–14].

The cellulosic fibers align to their length direction with minimal microfibril angles. Such alignment leads to a maximum tensile strength and provides the rigidity in the fiber direction. However, the length of the single cellulosic fiber used in wood fiber plastic composites is closer to a powder form with aspect ratios of 5 10. Because of their shorter fiber length, their reinforcement potential for the composites is limited [12, 15–17]. Increasing the length of the natural fibers obtained by a bacterial retting method is one of the alternatives to improve natural fiber reinforcement. Agricultural bast fibers obtained from jute, hemp, sisal, and

Correspondence to: Sangyeob Lee; e-mail: slee@cfr.msstate.edu
Contract grant sponsor: Department of Energy (Oak Ridge National Laboratory, ORNL; Center for Virtual Design and Manufacturing); contract grant number: DE-AC05-00OR22725.
DOI 10.1002/pc.20893
Published online in Wiley InterScience (www.interscience.wiley.com).

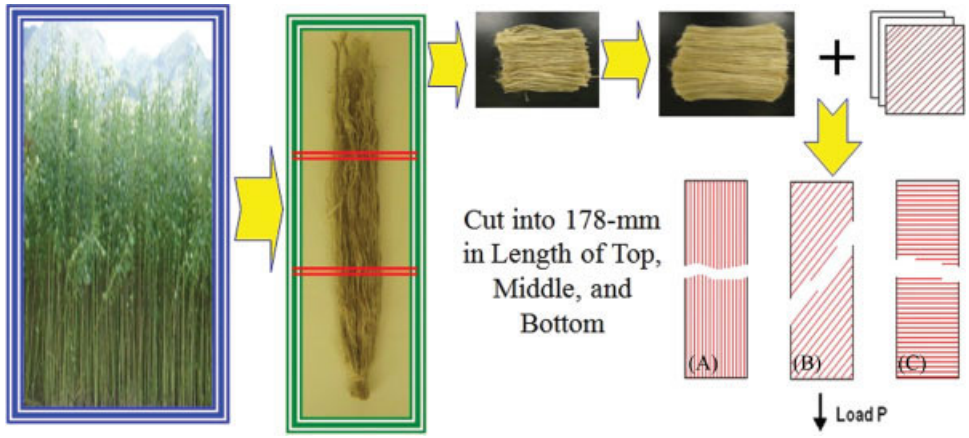

FIG. 1. Thirteen layers of laminate fabrication from raw materials to evaluate the effect of oriented angles. (A= 0°, B = 45°, and C = 90°).[Color figure can be in the online issue,which is available at www.interscience.wiley.com.]

kenaf can be good candidates because of their relatively high cellulose content and enhanced fiber properties [18–24]. Long kenaf (*Hibiscus cannabinus* L.) bast fiber bundles are traditionally used to make ropes, mats, carpets, paper, and other products [25]. In recent years, there has been an increasing interest in finding new applications of natural bast fibers in sheet molding compound (SMC) composites for automobile parts to replace synthetic fibers made of glass and carbon.

Most of the natural fibers are discontinuous. Thus, fiber contribution is insufficient to compare to mechanical properties of the continuous fiber reinforced composites [26]. Extensive studies have been carried out recently to better understand on the fiber orientation effect and single fiber characteristics on the mechanical property enhancement of composites. The objectives of this study were to evaluate kenaf bast fiber characteristics, to investigate the effect of fiber orientation on the mechanical properties of laminates, and to characterize the thermal and interfacial properties at the kenaf fiber and polymer interface.

EXPERIMENTAL

Materials

Stem-length kenaf fibers (*Hibiscus cannabinus*, L.) processed from a bacterial retting method, were obtained from The Golden Fibre Trade Centre Limited (GFTCL, Bangladesh). The bast fibers were conditioned at an ambient temperature of 22 ± 5°C and a relative humidity of 50 ± 5% until an equilibrium moisture content (EMC) of 8% was obtained. The stem-length fibers were macerated to obtain single fibers for property characterization. Hydrogen peroxide (H_2O_2) was used to macerate the kenaf fiber bundles.

Rolls of polypropylene film (PP: CO-EX Oriented Polypropylene), serving as the polymer matrix, were provided by Plastic Suppliers, Inc. Dallas, TX. The PP film was heat sealable, co-extruded, and biaxially oriented.

Laminated Natural Fiber–Polymer Composites Fabrication

Figure 1 shows the fabrication procedure of kenaf and polypropylene film laminates used in this study. Stem-length bacterial retted fibers were cut into a length of 178 mm and were straightened by combing. Laminates with a total of 13 layers (6 layers of kenaf fibers and 7 layers of PP films) were fabricated. The effects of fiber orientation angles (0°, 45°, 90° and random) and material formulations (kenaf/PP = 30/70, 40/60 and 50/50 in weight fractions) were investigated. Total 36 laminates were fabricated based on the four orientation angles, three material formulation, and three replicates. The laminates were placed into a PP film bag and heat sealed under a vacuum pressure of 1.4 kg·cm^{-2} in order to minimize the air captured in the composites during laminated natural fiber–polymer composite (LNPC) fabrication. A 152 × 152 mm^2 laboratory hot press was used to press the laminates. The laminates were processed at a pressure of 7.03 kg·cm^{-1} and a temperature of 200°C for 160 s. The compressed laminates were quickly cooled down at a rate of 25°C min^{-1}. The laminate samples were stored in an environment with an ambient temperature of 22°C for 24 hr before the mechanical test samples were prepared. The kenaf fiber bundles were also cut from three stem locations of top, middle, and bottom into 50-mm length. The fiber properties, such as single fiber length, diameter, surface topography, and surface roughness at the three locations were characterized and compared. In addition, sheet molding compound (SMC) mats reinforced by 25% fiberglass were provided by Meridian Automotive Systems (Grabill, IN) and served as positive controls for this experiment.

Instrumental and Data Collection

Tensile tests were conducted on the kenaf bast fiber bundles retted from the top, middle, and bottom of the kenaf stem using a mechanical tester, Mach1V500, CS instrument Inc. The loading capacity for this tester was

 DOI 10.1002/pc

10 N, and the accuracy of the load cell was ± 0.1 g at 0.5 μm displacement. Before and after testing, a Spot Insight Camera (Advanced V 4.6, Diagnostic Instrument, Sterling Heights, MI) was used for capturing images of the fiber bundles. The captured images were analyzed by using UTHSCSA Image Tool® V.3.0. Fiber lengths and diameters of bast fibers were collected from the images to characterize regional differences of kenaf fibers from 30 single fibers in each top, middle and bottom section. The characteristics of macerated kenaf fibers were also evaluated by using the image analysis system to determine the single fiber length and diameter.

Atomic force microscopy (AFM; Nanoscope IIIa – Digital Instruments, Veeco Metrology, Santa Barbara, CA) and scanning electron microscopy (SEM; Zeiss SupraTM 40 – Gemini®, Carl Zeiss MicroImaging, Thornwood, NY) were used to characterize the surface topography and morphology of bast fibers from top, middle, and bottom locations. Tapping mode was used in the AFM analysis. Two scanning areas, 2.5 × 2.5 μm^2 and 1 × 1 μm^2, were used to evaluate the differences in topography and root mean square (RMS) for surface roughness of the bast fiber bundles at top, middle and bottom sections of whole length kenaf stem. Fiber surface morphology and the fracture surface of laminates were examined using the SEM. The SEM micrographs were obtained at magnifications of 100 and 500× at a voltage of 5 kV.

Mechanical testing for the LNPC was conducted using Instron 5869 with a 5 kN load cell at a room temperature of 25°C. The crosshead speed was 6.4 mm·min^{-1} for tensile strength (TS) testing from ASTM D638-03 and 3.2 mm min^{-1} for the flexural testing (modulus of elasticity; MOE and modulus of rupture; MOR) based on the procedures described in ASTM D 790-96a. The cross section area of the tensile specimens was measured as 6.4 × 40.6 mm^2. An 8% elongation was obtained from the tensile strength measurement. The failure modes of the laminates were also observed as a function of the fiber orientation angles of 0°, 45°, 90°, and random orientations. Nine replicates per orientation angle were used in the testing.

Thermal analysis was carried out using the thermal gravimetry analysis with differential scanning calorimetry (TGA-DSC; Setsys Evolution 1750 TGA-DSC 150) and GC-MS (Setaram Instrumentation) under a nitrogen atmosphere (40 ml min^{-1}). The experiments followed the standard procedures described in ASTM E793-01 and E794-01. Thermal characteristics such as peak, onset temp, and heat flow were collected at a scan rate of 5 °C·min^{-1} heating (−25 to 200°C) and cooling (200 to 50°C).

RESULTS AND DISCUSSION

Mechanical and Physical Properties of Bundles and Single Fibers

The mechanical and physical properties of stem fibers are useful to predict the overall properties of composites. Table 1 shows the mechanical properties, surface roughness and fiber dimensions of the bacterial retted stem length kenaf fibers. The fibers were from top (50.8 mm from the top), bottom (50.8 mm from the bottom), and middle section (between the top and bottom sections) of the stem length of bacterial retted kenaf fibers. As shown in Table 1, the fiber bundles from the middle section yielded the highest Young's modulus and tensile strength compared to those from the other two sections. Both fiber lengths and diameters measured from this study were close to the previously published values around 12 μm [25]. Table 1 also showed that the surface roughness of the kenaf bundles decreased from the top to bottom section for the kenaf stem. In general, the bottom section of kenaf stems contained high lignin contents for stem support [25] while the kenaf fiber bundles from the top section contain more juvenile fibers with a lower fiber length. Thus, fiber bundles from middle section give the highest Young's modulus and tensile strength.

Figure 2 shows the morphological and topographical images of the bacterial retted kenaf fiber bundles obtained from top, middle and bottom sections. The SEM images generated with a magnification of 100× showed a relatively smooth surface of the fiber bundles. Deposited particles were clearly shown on the surface of the bacterial retted kenaf fibers for three fiber sections. The deposited materials on the fiber surface might be from the fractures of kenaf fibers generated during the retting process. The topographic images of the fiber surfaces at different height also showed a similar appearance. The height for the fibers from the middle section was 190 nm which was considered the smoothest surface among three sections. However, the differences in the surface roughness of each scan area showed a trend of reduced mean values from the top to bottom locations of the kenaf stem (Table 1).

Fiber Orientations and Material Types on the Mechanical Properties of the Laminates

Figure 3 showed that the MOE of the LNPC increased as the kenaf fiber contents increased when the fibers were oriented parallel to the load direction. Forty percent kenaf fiber content provided a higher strength for the composites compared to other mixing ratios. The fiber orientation angles played an important role on the mechanical property enhancement. The modulus and strength were decreased as the fiber angle increased. The 45° and 90° angles of fiber orientation provided less of a contribution to the flexural modulus and strength of LNPC regardless of the fiber content in the laminates. Usually, the strength of kenaf fibers contributes to an enhanced strength of the natural fiber reinforced composites. In this study, the differences in the composite properties between parallel and perpendicular fiber orientations were pronounced. The mechanical properties of the composites fabricated at 0° angle along the fiber direction were five to ten times higher than that with the orientation of 90°. This was also

TABLE 1. Kenaf fiber bundles and single fiber properties.

	Young's modulus[a] (GPa)	Tensile strength[a] (MPa)	Length[b] (mm)	Diameter[b] (μm)	Surface roughness (RMS) 2.5-μm Scan	Surface roughness (RMS) 1-μm Scan
Top	12.1 (2.0)	0.20 (0.05)	2.50 (0.72)	12.0 (1.5)	119.5 (114.1)	47.5 (29.9)
Middle	18.5 (3.4)	0.26 (0.10)	2.62 (0.58)	11.7 (1.3)	57.5 (19.1)	30.9 (15.8)
Bottom	13.5 (3.0)	0.17 (0.41)	2.79 (0.52)	12.3 (1.1)	54.6 (25.2)	26.1 (11.5)

RMS, root mean square.
[a] Averages of 25 Fiber Bundles. (Standard deviation).
[b] Measurement from 25 single fibers.

resulted from less matrix and lack of interfacial compatibility between surface of kenaf fibers and polyolefin matrix.

Figure 4 shows the flexural modulus and strength of LNPC affected by the fabrication types. The strength and stiffness data were obtained from composites with 40% kenaf fiber content at different fiber orientations. Composites made from pure PP matrix, wood flour/PP and kenaf fiber/PP with 90° fiber orientation showed lower mechanical properties. Composites with randomly oriented kenaf fiber reinforcement provided an equal or higher enhancement compared to fiber glass reinforcement in polyvinyl ester resin as a matrix. It is usually believed that the polypropylene matrix is weaker than the polyvinyl ester resin.

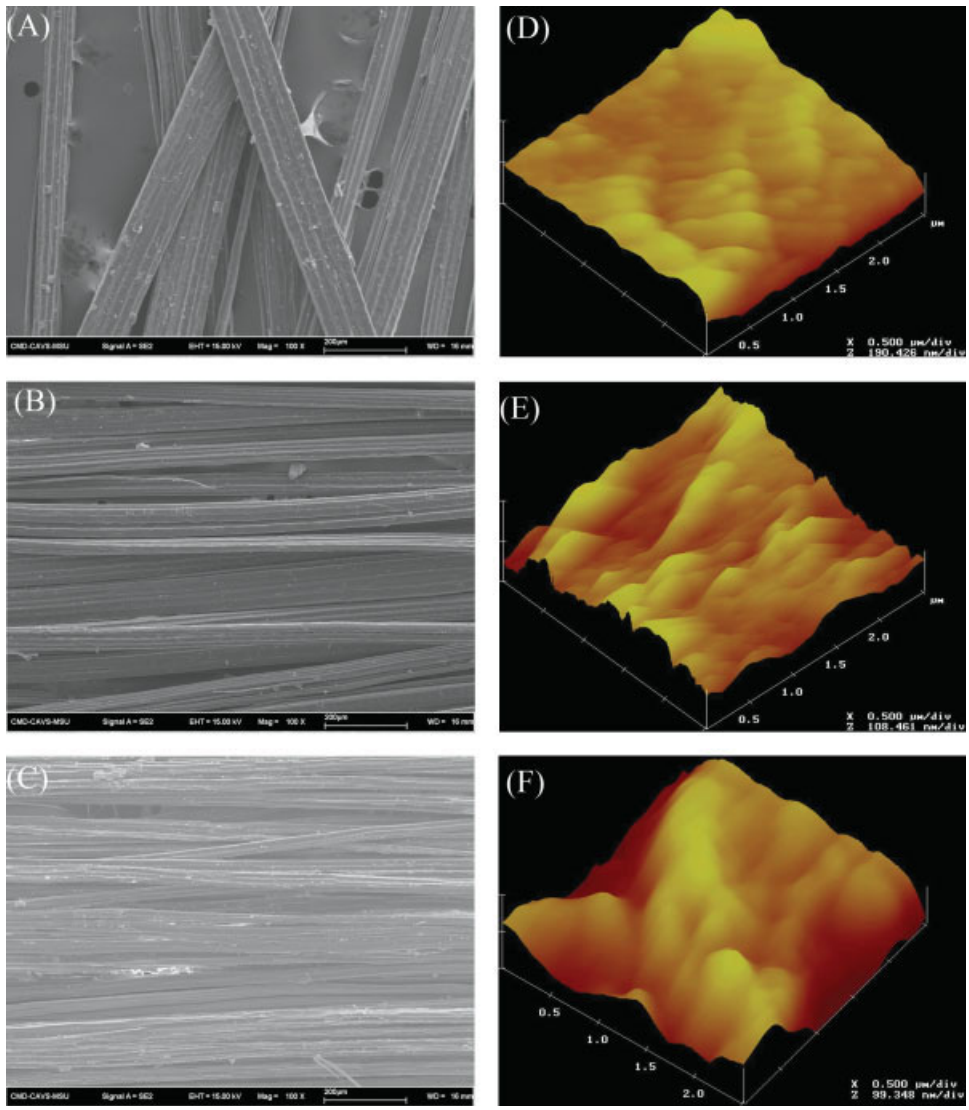

FIG. 2. Morphological (A = Top, B = Middle, and C = Bottom) and topographical (D = Top, E = Middle, and F = Bottom) images of kenaf bast fiber bundles produced by bacterial retting. [Color figure can be viewed in the online issue, which is available at www.interscience.wiley.com.]

 DOI 10.1002/pc

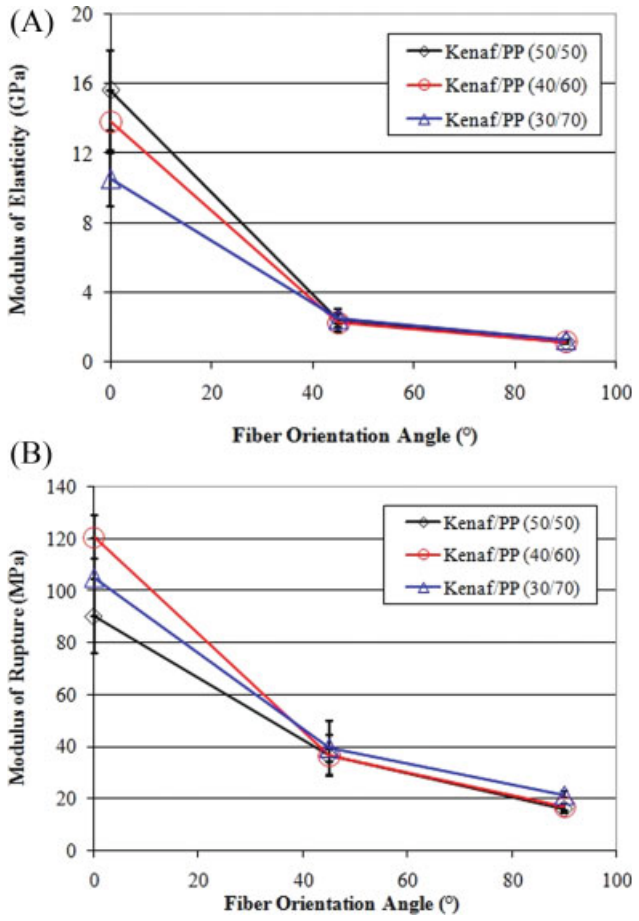

FIG. 3. Flexural modulus and strength of kenaf fiber and polypropylene (PP) film laminates as function of the different fiber orientation with three different kenaf and PP formulations. (A = Modulus of elasticity, B = Modulus of rupture, the error bar indicates one standard deviation). [Color figure can be viewed in the online issue, which is available at www.interscience.wiley.com.]

It is interesting to note that the failure modes of the two matrices under the applied stress differed. Composites made from SMC mats tended to a linear response to failure while LNPC was linear to curvilinear to the mechanical failure and tend to be more plastic.

Figure 5 shows the result of tensile strength (TS) of LNPC fabricated with 40% kenaf fibers and 60% PP film. The tensile strength of the laminates showed a similar trend to that of the flexural modulus and strength. The highest tensile strength was obtained for the composites with a 50% kenaf content and 0° fiber orientation. Reinforcement of tensile strength was less for the composites with the orientation angles of 45° and 90°. The tensile strength at 45° and 90° fiber orientation angle was much less than composites fabricated with the pure PP because of the lack of matrix contents and weakness at the fiber surface and matrix interface. The increased kenaf fiber contents resulted in an increased tensile strength when the fiber orientation was 0° Fig. 5a). The 0° orientation contributed mainly to the banding stuffiness and strength due to the orientation of the cellulose microfibrils along the axis of the load direction. In the comparison of fabrication types, composites made from kenaf fiber bundles of 25.4 mm in length at a random orientation obtained a compatible strength to the composites processed from SMC mats. It is encouraging to see that the random oriented kenaf fiber reinforcement has potential to provide equivalent properties as the fiber glass/polyvinyl ester composites under the current lab compression molding process.

The tensile failure modes of LNPC fabricated at different fiber orientations are showed in Fig. 6. The three fiber orientations showed significant difference in load transfer behaviors. Shear stress occurred along the initially preferred direction of fiber orientation angles. As shown in Fig. 5, composites made from highly oriented fiber bundles showed a higher shear stress at the fiber surface and matrixes Fig. 6a). Other fiber orientation angles were less effective in the stress transfer and yielded a poor enhancement on the mechanical properties. An important consequence of the failure process was a propensity for stress propagation along the dominant fiber orientation direction as 0°, 45°, and 90°. The different fiber angles

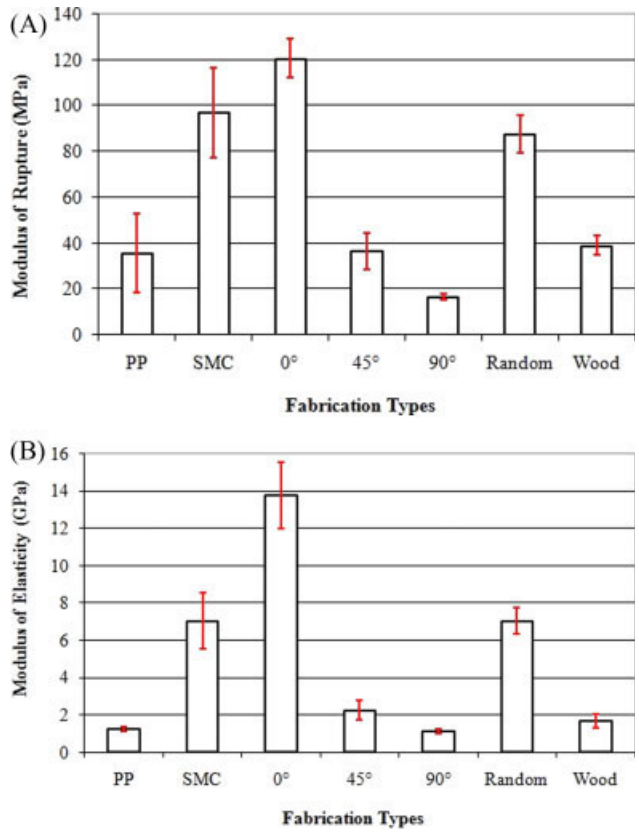

FIG. 4. Flexural modulus and strength of kenaf fiber and polypropylene (PP) film laminates as function of the different fiber orientation with three different kenaf and PP formulations. (A = Modulus of elasticity, B = Modulus of rupture, Fiber and matrix ratio = 40% Kenaf/60% PP, SMC = Fiber glass reinforced sheet molding compounds, Wood = 40 mesh wood flour, the error bar indicates one standard deviation). [Color figure can be viewed in the online issue, which is available at www.interscience.wiley.com.]

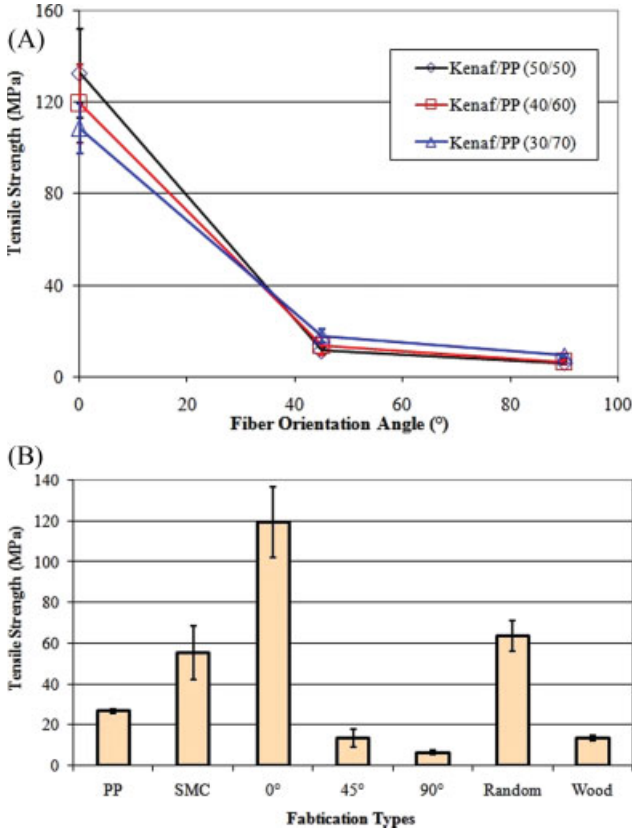

FIG. 5. Tensile strength of kenaf fiber and polypropylene (PP) film laminates. (A = Tensile strength at the different fiber orientation, B = Comparisons between fabrication types, Fiber and matrix ratio = 40% Kenaf/60% PP, SMC = fiber glass reinforced sheet molding compounds, Wood = 40 mesh wood flour, the error bar indicates one standard deviation). [Color figure can be viewed in the online issue, which is available at www.interscience.wiley.com.]

lead to failure in a relatively uniform tensile mode. Therefore, the different stress transfer behaviors and the lack of interfacial bonding may play an important role on the interfacial failure of LNPC. It should also be noticed that the randomly oriented kenaf fiber reinforcement in the composite was one of the promising way to obtain a comparable property enhancement without alignment effects in the LNPC fabrication.

Thermal Properties of Kenaf fiber/PP Formulations

Thermal characteristics of the prepared kenaf fiber–PP formulations were evaluated by TGA-DSC technique

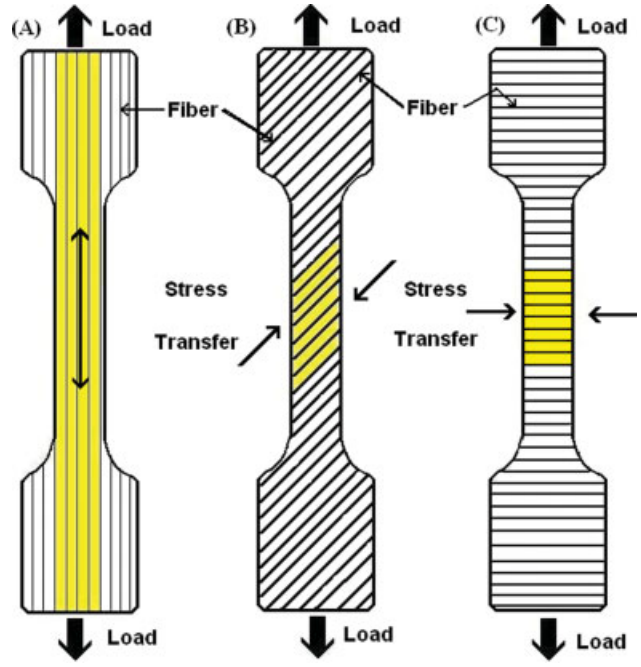

FIG. 6. Stress transfer along the continuous fiber directions oriented at 0°, 45°, and 90°. [Color figure can be viewed in the online issue, which is available at www.interscience.wiley.com.]

(Table 2). The TGA-DSC results provided information on the following thermo-physical properties of onset temperature, peak temperature and melting enthalpy. It is well known that the heat flow can act as an indicative tool for the dispersion state of the fillers in the natural fiber – polymer composites [5]. The polymer melting and maximum crystallization points with the addition of kenaf fibers were initiated earlier than that of the pure PP. An increased crystallization peak temperature was observed when the fibers were incorporated in the polymer matrices. This increment could be more sensitive when the fibers are chemically and physically modified [27, 28]. Thus, the fiber reinforcement influenced the thermal histories of the PP polymer such as increased heat flow and delayed polymer relaxation. The thermal property changes resulted in a higher enthalpy in both melting and crystallization. The increased heat of fusion and earlier induction of PP crystallization can be explained by the increased nucleation ability and crystallinity of the polymer matrices on the surface of retted kenaf fibers [5].

TABLE 2. Thermal characteristics of kenaf fiber and polypropylene formulations.

	Heating			Cooling		
	Onset temp. (°C)	Peak temp. (°C)	Enthalpy (μV s mg^{-1})	Onset temp. (°C)	Peak temp. (°C)	Enthalpy (μV s mg^{-1})
PP only	153.0	166.3	24.5	122.3	116.9	25.5
Kenaf/PP (50/50)	154.9	165.3	37.9	127.1	120.9	42.2
Kenaf/PP (40/60)	154.2	165.0	37.7	126.7	120.0	35.2
Kenaf/PP (30/70)	153.1	164.9	53.1	127.1	120.5	57.9

DOI 10.1002/pc

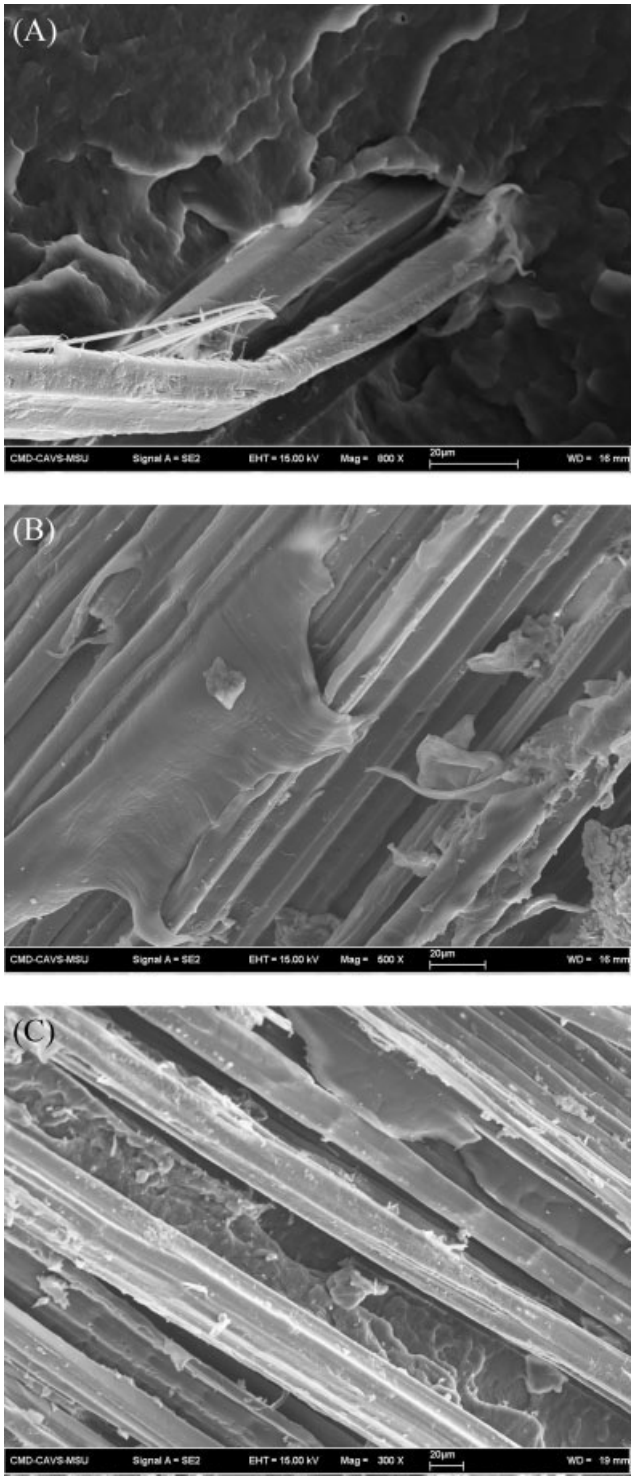

FIG. 7. Fractural morphology of kenaf bast fibers and polypropylene laminates. (Fiber orientation angles of A = 0°, B = 45°, and C = 90°).

Fractural Morphology at the Interface

A scanning electron microscope (SEM) image of fracture surfaces at the thermoplastic and kenaf fiber interface is shown in Fig. 7. A relatively uniform fiber distribution is shown in the PP matrix. Polymer melt flow was also shown among the reinforced kenaf fibers. The images also suggest that the fracture appeared to be dominated by the shear failure mode. The weak interfacial bonding between the kenaf fibers and polymer matrix indicated a poor compatibility at the interface. Inter laminar crack propagation at the hydrophobic and hydrophilic interface was observed in the kenaf fiber/PP composites. The kenaf fibers oriented along the fiber direction (Fig. 7a) were pulled out from the brittle PP matrix. For the other two fiber orientations, it is clearly showed that an interfacial failure and separation happened at the interface. The fiber bundles oriented at 45° angle were covered by the molten PP polymer matrix. Therefore, the failures at the interface with the stretched matrix under shear loads were observed. Failures appeared to be at the interface and matrix itself for those with the fibers oriented perpendicular to the applied stress direction. The interfacial failure initiates at the weak boundaries of the fiber surface and matrix interface. The composite starts to fail along the interface producing the local strains. A decreased property enhancement was resulted due to the interfacial failures. Fracture macrographs shown in Fig. 7 indicated a weak interaction and incompatibility at the kenaf fiber and PP interface.

In the micrographs (Fig. 7) of fracture surfaces, air pockets were hardly observed regardless of different fiber orientation angles. Minimized air pockets and controlling moisture contents of the kenaf fibers has been a challenge in the processing of natural-fiber polymer composites. Natural fibers are known as a hydrophilic nature with exposed hydroxyl end groups on the surface. In general, the fibers tend to reach the EMC of the surrounding environment. Usually, it is costly to dry natural cellulose fiber to less than 1% moisture content. During the polymer fabrication process, the moisture is captured at the inner structural of the fibers and prevents intimate contact at the natural fiber and polymer interface. Therefore, the control of moisture content in the fibers is a primary consideration in natural-fiber reinforced polymer composites. It has been showed that sisal fiber/polymer composites exposed under moisture conditions and resulted in a reduction of up to 50% in mechanical properties [4]. Therefore, the hollow structure of the stem length kenaf bast fibers may contribute a steamy transfer of residual moisture and prevent the moisture captured in the polymer composites.

CONCLUSIONS

The effects of fiber orientation on the mechanical properties of LNPC, kenaf bast fiber characteristics, and thermal/interfacial characteristics at kenaf fiber and polymer interface were investigated. Fibers from middle section of the kenaf stem showed relatively smoother surfaces and higher strength compared to those from other sections. The mechanical properties (MOE, MOR, and TS) increased as the fiber orientation angel decreased. The random oriented kenaf fiber reinforcement in PP showed

an equal property compared to that from fiber glass reinforcement in polyvinyl ester resin. Thermal properties were also altered with the presence of different weight fractions of kenaf fibers in the PP matrix. The fracture micrographs indicated a weak interaction at the interface of kenaf fiber surface and PP matrix.

REFERENCES

1. B. Mlekusch, E.A. Lehner, and W. Geymayer, *Compos. Sci. Technol.*, **59**, 543 (1999).
2. N. Chand and U.K. Dwivedi, *Polym. Compos.*, **28**(**4**), 437 (2007).
3. G.C. Jacob, J.M. Starbuck, J.F. Fellers, and S. Simunovic, *Polym. Compos.*, **26**, 293 (2005).
4. N.E. Zafeiropoulos, D.R. Williams, C.A. Baillie, and F.L. Matthews, *Compos. A*, **33**, 1083 (2002).
5. S.Y. Lee, Ph.D. Dissertation, Some Factors Affecting the Interfacial Interaction at Thermomechanical Fiber and Polypropylene Interphase, Louisiana State University, Baton Rouge, LA (2006).
6. S.A. Hashemi, H. Arabi, and N. Mirzaeyan, *Polym. Compos.*, **28**, 713 (2007).
7. D. Nabisaheb and J.P. Jog, *Adv. Polym. Technol.*, **18**, 351 (1999).
8. J. Holbery and D. Houston, JOM-J. *Miner. Met. Mater. Soc.*, **58**(**11**), 80 (2006).
9. Y. Xue, D.R. Veazie, C. Glinsey, M.F. Horstemeyer, and R.M. Rowell, *Compos. B*, **38**, 152 (2007).
10. C. Clemons, *Forest Prod. J.*, **52**(**6**), 10 (2002).
11. S. Serizawa, K. Inoue, and M. Iji, *J. Appl. Polym. Sci.*, **100**, 618 (2006).
12. T.P. Skourlis, K. Pochiraju, C. Chassapis, and S. Manoochehri, *Compos. B*, **29**, 309 (1998).
13. D.A. Norman and R.E. Robertson, *J. Appl. Polym. Sci.*, **90**, 2740 (2003).
14. R. Blanc, C. Germain, J.P. Da Costa, P. Baylou, and M. Cataldi, *Compos. A*, **37**, 197 (2006).
15. B. Feng, D.M. Cao, W.J. Meng, J. Xu, R.C. Tittsworth, L.E. Rehn, P.M. Baldo, and G.L. Doll, *Surf. Coat. Tech.*, **148**(**2–3**), 153 (2001).
16. L.M. Arzondo, A. Vazquez, J.M. Carella, and J.M. Pastor, *Polym. Eng. Sci.*, **44**(**9**), 1766 (2004).
17. K. Bledzki, H.P. Fink, and K. Specht, *J. Appl. Polym. Sci.*, **93**(**5**), 2150 (2004).
18. R. Karnani, M. Krishnan, and R. Narayan, *Polym. Engin. Sci.*, **37**(**2**), 476 (1997).
19. A.K. Rana, A. Mandal, B.C. Mitra, R. Jacobson, R. Rowell, and A.N. Banerjee, *J. Appl. Polym. Sci.*, **69**, 329 (1998).
20. S.J. Eichhorn, C.A. Baillie, N. Zafeiropoulos, L.Y. Mwaikambo, M.P. Ansell, A. Dufresne, K.M. Entwistle, P.J. Herrera-Franco, G.C. Escamilla, L. Groom, M. Hughes, C. Hill, T.G. Rials, and P.M. Wild, *J. Mater. Sci.*, **36**, 2107 (2001).
21. A.R. Sanadi, J.F. Hunt, D.F. Caulfield, G. Kovacsvolgyi, and B. Destree, "High Fiber-Low Matrix Composites: Kenaf Fiber/Polypropylene," in: 6th International Conference on Woodfiber-Plastic Composites, Madison, Wisconsin (2002).
22. K. Joseph, S. Thomas, C. Pavithran, and M. Brahmakumar, *J. Appl. Polym. Sci.*, **47**, 1731 (1993).
23. P.V. Joseph, K. Joseph, S. Thomas, C.K.S. Pillai, V.S. Prasad, G. Groeninckx, and M. Sarkissova, *Compos. A.*, **34**, 253 (2003).
24. M. Tajvidi, R.H. Falk, and J.C. Hermanson, *J. Appl. Polym. Sci.*, **97**, 1995 (2005).
25. T. Sellers and N.A. Reichert, *Kenaf Properties, Processing and Products*, Mississippi State University, Ag and Bio Engineering, Starkville (1999).
26. B. Nystrom, R. Joffe, and R. Langstrom, *J. Reinforced Plast. Compos.*, **26**(**6**), 579 (2007).
27. S. Lee, T.F. Shupe, L.H. Groom, and C.Y. Hse, *Wood Fiber Sci.*, **39**(**3**), 424 (2007).
28. S. Lee, T.F. Shupe, and C.Y. Hse, *Compos. Interfaces*, **15**(**2–3**), 221 (2008).
29. M. Zampaloni, F. Pourboghrat, S.A. Yankovich, B.N. Rodgers, J. Moore, L.T. Drzal, A.K. Mohanty, and M. Misra, *Compos. A*, **38**, 1569 (2007).

 DOI 10.1002/pc